Available online at www.sciencedirect.com

ScienceDirect

IFAC PapersOnline CONFERENCE PAPER ARCHIVE

IFAC PapersOnLine 55-20 (2022) 151–156

Parametric Reduced-Order Modeling of Aeroelastic Systems

Tea Vojković * **Pierre Vuillemin** ** **David Quero** *
Charles Poussot-Vassal **

* *DLR (German Aerospace Center), Institute of Aeroelasticity, Göttingen 37073, Germany (e-mail: Tea.Vojkovic@dlr.de, David.QueroMartin@dlr.de).*
** *ONERA/DTIS, Toulouse 31055, France (e-mail: Pierre.Vuillemin@onera.fr, Charles.Poussot-Vassal@onera.fr).*

Abstract:
In this paper, two approaches for modeling parameter-dependent unsteady aerodynamic loads for control design purposes are presented. The approaches are based on parametric Loewner frameworks, namely, transfer matrix interpolation and global basis. Combined with post-processing techniques, these frameworks generate highly accurate, reduced-order state-space models of aerodynamic loads. The approaches are computationally efficient since they can model the entire flight envelope while requiring only a single input set of aerodynamic transfer matrix data. Additionally, constant numerical settings can be used across wide ranges of the parameter values without loss of accuracy. The proposed approaches are applied to state-space modeling of a two-dimensional aeroelastic system. The evaluated accuracy and dynamic behavior of the model show excellent agreement with the reference frequency domain solutions for both approaches.

Keywords: Unsteady aerodynamics, state-space models, Loewner framework, aeroelastic systems, reduced-order modeling

1. INTRODUCTION

Transport aircraft design is mainly dictated by airworthiness specifications, regulated by aerospace agencies (EASA (2015)), as well as environmental and economic issues. Thus, one of the major priorities in the modern aerospace industry is the innovation to enhance aircraft performance, efficiency, and durability. Part of this effort is the development of next-generation active control systems, capable of reducing peak loads induced by atmospheric disturbances and manoeuvres as well as avoiding aeroelastic instabilities in flexible structures. This is of crucial importance if lighter structures with longer fatigue life and greater flight velocities want to be achieved.

The challenge of designing active control systems lies in casting flexible aircraft equations of motion in a form convenient for control analysis, namely the state-space form. For the optimal control design purposes, it is desired that the aeroelastic state-space models are accurate, time efficient, and of low order. The latter, however, is not achievable if unsteady aerodynamic loads are obtained with high-fidelity CFD solvers which require very fine spatial discretizations. Furthermore, if the flow around the system is described with potential flow theories, unsteady aerodynamic loads are either given as transcedental functions or as discrete values in the frequency domain, which cannot readily be used to formulate the state-space models. Therefore, to obtain the aeroelastic state-space models of low-order, adequate modeling of unsteady aerodynamic loads is needed. Due to the dependency of airloads on flight conditions, an accurate parametric model of low-order which covers the complete flight envelope while requiring a small set of computationally expensive input data is sought.

Historically, modeling of unsteady aerodynamic loads for control design purposes was first done by means of rational function approximation (RFA) methods (Roger (1977), Irving (1979)). The idea behind the RFA methods is to approximate the aerodynamic transfer matrix with a rational matrix in the Laplace (complex) domain which allows the formulation of aeroelastic state-space models. However, these methods introduce approximation errors in the description of the airloads and can suffer from numerical instabilities or require iterative procedures. To overcome these limitations, new approaches based on realization methods have been developed. Realization methods are used to identify the aerodynamic state-space matrices directly from sampled aerodynamic data which combined with structural matrices can form the aeroelastic state-space models. An approach based on general realization theory, namely the Loewner framework (Mayo and Antoulas (2007)), is proposed in Quero et al. (2019). This approach is particularly convenient since it generates reduced-order state-space models while introducing small approximation errors and requiring no iterative procedures. Quero's approach has been extended in the work of Vojković (2021) to account for parametric dependency of the airloads, using three different parametric Loewner frameworks developed in Ionita and Antoulas

10.1016/j.ifacol.2022.09.087

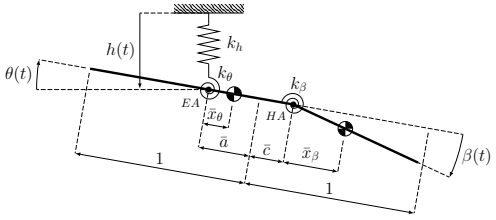

Fig. 1: Aeroelastic system with three degrees of freedom, namely, heave $h(t)$, pitch $\theta(t)$, and flap deflection $\beta(t)$. The positive direction of $h(t)$ is downwards. Distances are non-dimensionalized with half-chord length b. Note that $\bar{x}_\beta$ is not a physical distance but a reduced parameter. EA denotes the elastic axis and HA denotes the hinge axis.

(2014) and Yue et al. (2019). This extension improves the time efficiency of the approach by requiring a single set of input data for the whole flight envelope.

In this work, two approaches for generating state-space realizations of parameter-dependent aerodynamic loads presented in Vojković (2021), namely the transfer matrix interpolation and the global basis (Yue et al. (2019)), are used. The approaches are modified to achieve higher robustness and applied to aeroelastic state-space modeling. The paper consists of five sections. In Section 2, a flexible aircraft wing model and the procedure for constructing its state-space formulation are presented. Section 3 summarizes the Loewner framework which is the foundation of the approaches for unsteady aerodynamic modeling, presented in Section 4. Finally, in Sections 5, performances of the constructed aerodynamic and aeroelastic state-space models are evaluated.

2. AEROELASTIC SYSTEM

First, let us present the considered aeroelastic benchmark model together with the approach taken to construct its state-space formulation.

Structural model: The typical section of a flexible wing equipped with a trailing edge control surface, modeled as a flat plate with a flap (Fig. 1), is considered. The system has three degrees of freedom, namely, heave $h(t)$, pitch $\theta(t)$, and flap deflection $\beta(t)$. The latter is controlled by a motor which can apply a torque $T(t)$ around the hinge axis. Total wing mass per unit span length is denoted as m while the bending, torsional, and control surface hinge stiffness (per unit span length) are k_h, k_θ, and k_β, respectively. The distances of the elastic axis and the hinge axis, $\bar{a}$ and $\bar{c}$, are measured from the mid-chord and normalized with the semi-chord length b. The center of the total wing mass is located at the non-dimensional distance $\bar{x}_\theta$ behind the elastic axis, while the reduced distance of the control surface mass center from the hinge axis is $\bar{x}_\beta = S_\beta/(mb)$ (where S_β is a static moment of the control surface about the hinge axis per unit span length). Finally, I_θ and I_β denote the moment of inertia of the wing about the elastic axis and the moment of inertia of the control surface about the hinge axis per unit span length.

Aerodynamic model: The described structural model is immersed in the uniform, compressible flow with the velocity U and density ρ. Unsteady aerodynamic loads generated by structural displacements are calculated with a linear potential solver based on the Possio's integral equation (Marques (2019)). Within this solver, the plate is divided into n_p panels and the flow is modeled with discrete doublets placed at 3/4 length of each panel. This discretized Possio's equation is then solved for an unknown pressure distribution in the frequency domain by evaluating the Possio kernel and prescribing downwash velocities at collocation points. Finally, discrete values of the aerodynamic transfer matrix $\mathbf{H}_a(\imath k, M)$ which maps the structural and control surface displacements to aerodynamic load coefficients, lift $\hat{c}_l(\imath k, M)$, pitching moment about the elastic axis $\hat{c}_{m\theta}(\imath k, M)$, and moment about the hinge axis $\hat{c}_{m\beta}(\imath k, M)$,

$$\begin{bmatrix} \hat{c}_l(\imath k, M) \\ \hat{c}_{m\theta}(\imath k, M) \\ \hat{c}_{m\beta}(\imath k, M) \end{bmatrix} = \mathbf{H}_a(\imath k, M) \begin{bmatrix} \hat{h}(\imath k)/b \\ \hat{\theta}(\imath k) \\ \hat{\beta}(\imath k) \end{bmatrix},$$

are obtained. Due to compressibility of the flow, the aerodynamic transfer matrix depends on the reduced frequency k, defined as $k = (\omega b)/U$ (where ω is the angular frequency) and the Mach number M. However, to capture the dependency on other parameters such as Reynolds number and steady angle of attack, high fidelity solvers are needed. The sufficient number of panels needed to capture the behavior at high reduced frequencies, $n_p = 100$, is determined by comparing the aerodynamic transfer matrix values at $M = 10^{-6}$ with the analytical results given in Theodorsen (1935). The transfer matrix is calculated for a set of reduced frequencies and Mach numbers, where the minimum Mach number is $M = 0.1$ and the maximum Mach number is $M = 0.7$. These limits are chosen to avoid regions outside of the typical flight envelope for a transport aircraft, as well as the transonic regime which is not modeled correctly with inviscid flow theories.

Aeroelastic model: Dynamic behavior of the modeled flexible structure is influenced by structural dynamics, control surface motion, aerodynamics, and loads generated by control systems. This is accounted for in the linearized equation of motion (EOM), given in the time domain for the considered two-dimensional system as:

$$\mathbf{M}_s \ddot{\boldsymbol{\xi}}(t) + \mathbf{K}_s \boldsymbol{\xi}(t) = \mathbf{Q}_a(t, M) + [0\ 0\ 1]^T \bar{T}(t). \quad (1)$$

Here, $\boldsymbol{\xi}(t)$ is a vector of non-dimensional structural and control surface displacements, $\boldsymbol{\xi}(t) = [h(t)/b\ \theta(t)\ \beta(t)]^T$, and $\mathbf{Q}_a(t, M)$ is a vector of appropriately scaled aerodynamic load coefficients given in the time domain,

$$\mathbf{Q}_a(t, M) = \frac{\kappa U^2}{\pi b^2} \left[-c_l(t, M)\ 2c_{m\theta}(t, M)\ 2c_{m\beta}(t, M)\right]^T,$$

where $\kappa = (\pi \rho b^2)/m$ and $\bar{T}(t) = T(t)/(mb^2)$. Structural mass and stiffness matrices, $\mathbf{M}_s$ and $\mathbf{K}_s$, are:

$$\mathbf{M}_s = \begin{bmatrix} 1 & \bar{x}_\theta & \bar{x}_\beta \\ \bar{x}_\theta & r_\theta^2 & r_\beta^* \\ \bar{x}_\beta & r_\beta^* & r_\beta^2 \end{bmatrix},\ \mathbf{K}_s = \begin{bmatrix} \omega_h^2 & 0 & 0 \\ 0 & (r_\theta \omega_\theta)^2 & 0 \\ 0 & 0 & (r_\beta \omega_\beta)^2 \end{bmatrix},$$

where $r_\theta = \sqrt{I_\theta/(mb^2)}$, $r_\beta = \sqrt{I_\beta/(mb^2)}$, $r_\beta^* = r_\beta^2 + (\bar{c} - \bar{a})\bar{x}_\beta$, $\omega_h = \sqrt{(k_h/m)}$, $\omega_\theta = \sqrt{(k_\theta/I_\theta)}$, and $\omega_\beta = \sqrt{(k_\beta/I_\beta)}$. Structural parameters are set to the standard values used in Theodorsen (1935): $\bar{a} = -0.2$, $\bar{c} = 0.6$, $\bar{x}_\theta = 0.2$, $\bar{x}_\beta = 0.002$, $r_\theta = \sqrt{0.5}, \kappa = 0.083$, $r_\beta = \sqrt{0.02}$, $\omega_h = 60.7$ [rad/s], $\omega_\theta = 100$ [rad/s], $\omega_\beta/(mb^2) = 90$ [rad/s], $b = 0.5$ [m]. For an aeroelastic system to be stable, freestream

velocity U needs to be below the flutter boundary. Thus, U is set to 50% of the flutter speed for each Mach number, calculated with the $p-L$ method developed in Quero et al. (2021).

State-space model: To enable the future design of a control law for the observed aeroelastic model, the EOM given with Eq. 1 is brought to the linear, time-invariant (LTI) state-space form. This form is given as a set of ordinary differential equations (ODEs),

$$S_{ae}(p): \begin{array}{l} \dot{\mathbf{x}}_{ae}(t) = \mathbf{A}_{ae}(p)\mathbf{x}_{ae}(t) + \mathbf{B}_{ae}(p)\mathbf{u}_{ae}(t) \\ \mathbf{y}_{ae}(t) = \mathbf{C}_{ae}(p)\mathbf{x}_{ae}(t) + \mathbf{D}_{ae}(p)\mathbf{u}_{ae}(t), \end{array} \tag{2}$$

where $\mathbf{A}_{ae}(p), \mathbf{B}_{ae}(p), \mathbf{C}_{ae}(p), \mathbf{D}_{ae}(p)$ are the state-space matrices, $\mathbf{x}_{ae}(t)$ is the state vector while $\mathbf{u}_{ae}(t)$ and $\mathbf{y}_{ae}(t)$ are the input and output vector, respectively. For some structural model (fixed structural parameters), the system $S_{ae}(p)$ depends solely on the Mach number, $p = M$. In this work, the non-dimensional torque applied by the actuator is the input vector, $\mathbf{u}_{ae}(t) = \bar{T}(t)$, and the vector of non-dimensional structural and control surface displacements is the output vector, $\mathbf{y}_{ae}(t) = \boldsymbol{\xi}(t)$. This formulation enables direct control of the system's dynamics through the input vector as well as the evaluation of the system's behavior. However, state-space matrices, which consist of both structural matrices and aerodynamic loads, cannot be formulated directly from the EOM (Eq. 1). This is because the calculated tabular values of aerodynamic loads cannot be expressed as explicit functions of $\boldsymbol{\xi}(t)$ in the time domain. Therefore, aerodynamic load coefficients are modeled with the aerodynamic state-space system $S_a(M)$,

$$S_a(M): \begin{array}{l} \dot{\mathbf{x}}_a(t) = \dfrac{U}{b}\mathbf{A}_a(M)\mathbf{x}_a(t) + \mathbf{B}_a(M)\mathbf{u}_a(t) \\ \mathbf{Q}_a(t,M) = \dfrac{U}{b}\mathbf{C}_a(M)\mathbf{x}_a(t) + \mathbf{D}_a(M)\mathbf{u}_a(t), \end{array} \tag{3}$$

where

$$\mathbf{B}_a(M) = [\mathbf{B}_{a0}(M)\ \mathbf{0}\ \mathbf{0}],\ \mathbf{u}_a(t) = \left[\boldsymbol{\xi}(t)\ \dot{\boldsymbol{\xi}}(t)^T\ \ddot{\boldsymbol{\xi}}(t)^T\right]^T,$$
$$\mathbf{D}_a(M) = \left[\mathbf{D}_{a0}(M)\ (U/b)\mathbf{D}_{a1}(M)\ (U/b)^2\mathbf{D}_{a2}(M)\right],$$

and $\mathbf{x}_a(t)$ is referred to as the aerodynamic lag state vector. Using the two approaches based on the Loewner framework, presented in Section 3, aerodynamic state-space matrices $(\mathbf{A}_a, \mathbf{B}_a, \mathbf{C}_a, \mathbf{D}_a)(M)$ can be identified for any Mach number from a single set of scaled transfer matrix data, $\tilde{\mathbf{H}}_a(\imath k, M) = (\kappa U^2/\pi b^2) \cdot \mathrm{diag}(-1, 2, 2)\mathbf{H}_a$, calculated along discrete sample points for k and M. The associated transfer matrix of the system S_a, $\tilde{\mathbf{H}}(S_a)(\bar{s}, M) = \mathbf{C}_a(M)(\bar{s}\mathbf{I} - \mathbf{A}_a)^{-1}\mathbf{B}_{a0}(M) + \mathbf{D}_{a2}(M)\bar{s}^2 + \mathbf{D}_{a1}(M)\bar{s} + \mathbf{D}_{a0}(M)$, is a rational matrix of the non-dimensional complex variable $\bar{s} = (sb)/U$, where the complex variable s is $s = \zeta + \imath\omega$ and ζ is the damping coefficient. The goal is to obtain $\tilde{\mathbf{H}}(S_a)(\bar{s}, M)$ such that it closely approximates the sampled transfer matrix data, $\tilde{\mathbf{H}}(S_a)(\imath k, M) \approx \tilde{\mathbf{H}}_a(\imath k, M)$. Once the aerodynamic state-space matrices are identified, the aeroelastic state-space model (Eq. 2) is formulated by inserting Eq. 3 into Eq. 1. Finally, defining the state variable, input, and output vector as $\mathbf{x}_{ae}(t) = \left[\boldsymbol{\xi}(t)^T\ \dot{\boldsymbol{\xi}}(t)^T\ \boldsymbol{x}_a(t)^T\right]^T$, $\mathbf{u}_{ae}(t) = \bar{T}(t)$, and $\mathbf{y}_{ae}(t) = \boldsymbol{\xi}(t)$, the associated aeroelastic state-space matrices follow:

$$\mathbf{A}_{ae}(M) = \begin{bmatrix} \mathbf{0} & \mathbf{I} & \mathbf{0} \\ -\bar{\mathbf{M}}^{-1}\bar{\mathbf{K}} & -\bar{\mathbf{M}}^{-1}\bar{\mathbf{C}} & \bar{\mathbf{M}}^{-1}\mathbf{C}_a \\ \mathbf{B}_{a0} & \mathbf{0} & \mathbf{A}_a \end{bmatrix},\ \mathbf{C}_{ae} = [\mathbf{I}\ \mathbf{0}\ \mathbf{0}],$$

$$\mathbf{B}_{ae}(M) = \begin{bmatrix} \mathbf{0} \\ \bar{\mathbf{M}}^{-1}\begin{bmatrix}0\\0\\1\end{bmatrix} \\ \mathbf{0} \end{bmatrix},\ \mathbf{D}_{ae} = \mathbf{0},$$

where $\bar{\mathbf{M}} = \mathbf{M}_s - \mathbf{D}_{2a}$, $\bar{\mathbf{C}} = -\mathbf{D}_{a1}$ and $\bar{\mathbf{K}} = \mathbf{K}_s - \mathbf{D}_{a0}$.

Using the described procedure, we construct aerodynamic and aeroelastic state-space models of low orders (small sizes of the state vectors) for the observed range of Mach numbers. Prior to discussing the unsteady aerodynamic modeling, an overview of the Loewner framework is given.

3. GENERALIZED REALIZATION IN THE LOEWNER FRAMEWORK

3.1 Generalized realization problem

In the generalized realization theory, a set of transfer function/matrix data sampled at N values of the complex variable s (here assumed to be distinct),

$$\{s_i, \boldsymbol{\Phi}_i \mid s_i \in \mathbb{C}, \boldsymbol{\Phi}_i \in \mathbb{C}^{n_y \times n_u}\}, \quad i = 1:N, \tag{4}$$

where n_u and n_y are the number of inputs and outputs, is modeled with a generalized state-space system or descriptor system Σ,

$$\Sigma: \mathbf{E}\dot{\mathbf{x}}(t) = \mathbf{A}\mathbf{x}(t) + \mathbf{B}\mathbf{u}(t),\ \mathbf{y}(t) = \mathbf{C}\mathbf{x}(t) + \mathbf{D}\mathbf{u}(t). \tag{5}$$

Here, $\mathbf{x}(t) \in \mathbb{R}^n$ denotes the internal variable of order (size) n, $\mathbf{u}(t) \in \mathbb{R}^{n_u}$ is the input vector, $\mathbf{y}(t) \in \mathbb{R}^{n_y}$ is the output vector while $\mathbf{A}, \mathbf{E} \in \mathbb{R}^{n\times n}$, $\mathbf{B} \in \mathbb{R}^{n\times n_u}$, $\mathbf{C} \in \mathbb{R}^{n_y\times n}$, $\mathbf{D} \in \mathbb{R}^{n_y\times n_u}$ are constant matrices. Generalization of the realization problem implies that the matrix $\mathbf{E}$ is allowed to be singular. The transfer function/matrix of the system Σ, $\tilde{\mathbf{H}}(\Sigma)(s) = \mathbf{C}(s\mathbf{E} - \mathbf{A})^{-1}\mathbf{B} + \mathbf{D}$, is a rational function/matrix, fully defined with the quintuple of matrices ($\mathbf{E}$, $\mathbf{A}$, $\mathbf{B}$, $\mathbf{C}$, $\mathbf{D}$) which is referred to as the realization of $\tilde{\mathbf{H}}(\Sigma)(s)$. We will not distinguish between Σ and ($\mathbf{E}$, $\mathbf{A}$, $\mathbf{B}$, $\mathbf{C}$, $\mathbf{D}$). Depending on the behavior at infinity, $\tilde{\mathbf{H}}(\Sigma)(s)$ can be strictly-proper ($\lim_{s\to\infty}\tilde{\mathbf{H}}(\Sigma)(s) = \mathbf{0}$), proper ($\lim_{s\to\infty}\tilde{\mathbf{H}}(\Sigma)(s) = const.$), and improper ($\lim_{s\to\infty}\tilde{\mathbf{H}}(\Sigma)(s) = \infty$). The realization of $\tilde{\mathbf{H}}(\Sigma)(s)$ is not unique, however, it is required that $\det(s\mathbf{E} - \mathbf{A}) \neq 0$, except for the finite number of generalized eigenvalues $\Lambda(\mathbf{A}, \mathbf{E})$. The system is completely controllable and observable when the order of realization n is minimal. For the minimal realizations, the poles of $\tilde{\mathbf{H}}(\Sigma)(s)$ are equal to the generalized eigenvalues $\Lambda(\mathbf{A}, \mathbf{E})$. The system Σ is asymptotically stable if $\Lambda(\mathbf{A}, \mathbf{E})$ are restricted to the left half of the complex plane, $\Re(\Lambda(\mathbf{A}, \mathbf{E})) < 0$. The system Σ models the data set accurately if the pointwise error matrices, $\mathbf{E}_{rr}(s_i) = \tilde{\mathbf{H}}(\Sigma)(s_i) - \boldsymbol{\Phi}_i$, have small norms.

3.2 Review of non-parametric Loewner framework

In the Loewner framework, sampled data is interpolated via Lagrange rational interpolation, and the minimal generalized realization of the rational interpolant is constructed directly from the sampled set by means of Loewner and shifted Loewner matrices. In the case of matrix data, the minimality of realization is achieved by tangential interpolation. The framework also allows for order reduction of the realization with the introduction of small approximation errors.

Sampled complex data given with Eq. 4 is partitioned into two disjoint sets,

$$\{\lambda_j, \mathbf{w}_j, j = 1 : n_r\} \cup \{\mu_i, \mathbf{v}_i, i = 1 : n_l\},$$

where $n_r + n_l = N$. In the tangential interpolation problem, rational interpolant $\tilde{\mathbf{H}}(s)$ needs to satisfy the following tangential constraints,

$$\tilde{\mathbf{H}}(\lambda_j)\mathbf{r}_j = \tilde{\mathbf{w}}_j, \quad \boldsymbol{\ell}_i\tilde{\mathbf{H}}(\mu_i) = \tilde{\mathbf{v}}_i, \tag{6}$$

where $\mathbf{r}_j \in \mathbb{C}^{n_u \times 1}$ and $\boldsymbol{\ell}_i \in \mathbb{C}^{1 \times n_y}$ denote the right and left tangential directions while $\tilde{\mathbf{w}}_j = \mathbf{w}_j\mathbf{r}_j$ and $\tilde{\mathbf{v}}_i = \boldsymbol{\ell}_i\mathbf{v}_i$ are the right and left tangential data. Tangential data can be written in the following matrix form:

$$\begin{aligned} \boldsymbol{\Lambda} &= \operatorname{diag}(\lambda_1, ..., \lambda_{n_r}), \quad & \mathbf{M} &= \operatorname{diag}(\mu_1, ..., \mu_{n_l}), \\ \mathbf{W} &= [\tilde{\mathbf{w}}_1 \ \dots \ \tilde{\mathbf{w}}_{n_r}], & \mathbf{V}^* &= \begin{bmatrix} \tilde{\mathbf{v}}_1^* \ \dots \ \tilde{\mathbf{v}}_{n_l}^* \end{bmatrix}, \\ \mathbf{R} &= [\mathbf{r}_1 \ \dots \ \mathbf{r}_{n_r}], & \mathbf{L}^* &= \begin{bmatrix} \boldsymbol{\ell}_1^* \ \dots \ \boldsymbol{\ell}_{n_l}^* \end{bmatrix}. \end{aligned}$$

The minimal realization of $\tilde{\mathbf{H}}(s)$, $\tilde{\mathbf{H}}(s) = \mathbf{C}(s\mathbf{E} - \mathbf{A})^{-1}\mathbf{B}$, is found by constructing the Loewner and shifted Loewner matrix, $\mathbb{L} \in \mathbb{C}^{n_l \times n_r}$ and $\mathbb{L}_\sigma \in \mathbb{C}^{n_l \times n_r}$,

$$[\mathbb{L}]_{ij} = \frac{\tilde{\mathbf{v}}_i\mathbf{r}_j - \boldsymbol{\ell}_i\tilde{\mathbf{w}}_j}{\mu_i - \lambda_j}, \quad [\mathbb{L}_\sigma]_{ij} = \frac{\mu_i\tilde{\mathbf{v}}_i\mathbf{r}_j - \boldsymbol{\ell}_i\tilde{\mathbf{w}}_j\lambda_j}{\mu_i - \lambda_j},$$

directly from the sampled data. Both Loewner matrices satisfy the Sylvester equation, $\boldsymbol{\Psi}\boldsymbol{\Lambda} - \mathbf{M}\mathbb{L} = \boldsymbol{\Psi}\mathbf{W} - \mathbf{V}\mathbf{R}, \boldsymbol{\Psi} \in \{\mathbb{L}, \mathbb{L}_\sigma\}$. One of the main observations in Mayo and Antoulas (2007) is that the rank of $\mathbb{L}$ and the Loewner pencil $(\mathbb{L}_\sigma, \mathbb{L})$, constructed from rational matrix samples, can reveal the McMillan degree q of the sampled rational matrix and the order of its minimal realization. Finding the minimal realization $(\mathbf{E}, \mathbf{A}, \mathbf{B}, \mathbf{C}, \mathbf{D})$ with $\mathbf{D} = \mathbf{0}$ relies on the following assumption:

$$\operatorname{rank}(s_i\mathbb{L} - \mathbb{L}_\sigma) = \operatorname{rank}[\mathbb{L} \ \mathbb{L}_\sigma] = \operatorname{rank}\begin{bmatrix} \mathbb{L}^* \ \mathbb{L}_\sigma^* \end{bmatrix}^* = n,$$

where $n = q + \min(n_u, n_y)$ is the minimal order of the system. This holds for sufficiently large data sets, $\min(n_l, n_r) \geq n$, which do not contain eigenvalues of $(\mathbb{L}_\sigma, \mathbb{L})$ and for generically chosen, linearly independent tangential directions (which form full-rank $\mathbf{R}$ and $\mathbf{L}$ matrices). Thus, the minimal realization of $\tilde{\mathbf{H}}(s)$ which satisfies the tangential constraints (Eq. 6) is given as:

$$\mathbf{E} = -\mathbf{Y}^*\mathbb{L}\mathbf{X}, \ \mathbf{A} = -\mathbf{Y}^*\mathbb{L}_\sigma\mathbf{X}, \ \mathbf{B} = \mathbf{Y}^*\mathbf{V}, \ \mathbf{C} = \mathbf{W}\mathbf{X} \tag{7}$$

where $\mathbf{Y} \in \mathbb{C}^{n_l \times n}$ and $\mathbf{X} \in \mathbb{C}^{n_r \times n}$ are the matrices containing the left and right singular vectors of $(\mathbb{L}_\sigma, \mathbb{L})$, $s_i\mathbb{L} - \mathbb{L}_\sigma = \mathbf{Y}\boldsymbol{\Sigma}\mathbf{X}^*$. The realization given with Eq. 7 holds for systems with an arbitrary number of inputs and outputs as well as improper, proper and strictly-proper transfer matrices. Note that here, due to space limitation, the procedure for avoiding complex realization (see Ionita (2013)) is omitted. However, when sampled data does not originate from a rational matrix, the Loewner pencil is usually full-rank. In that case, the minimal realization is given with:

$$\mathbf{E} = -\mathbb{L}, \ \mathbf{A} = -\mathbb{L}_\sigma, \ \mathbf{B} = \mathbf{V}, \ \mathbf{C} = \mathbf{W}, \tag{8}$$

and its order depends on the sample size. It is possible to reduce the order of model by projecting it onto the $\hat{n}$ most dominant left and right singular vectors of $(\mathbb{L}_\sigma, \mathbb{L})$, $\hat{\mathbf{Y}} \in \mathbb{C}^{n_l \times \hat{n}}$ and $\hat{\mathbf{X}} \in \mathbb{C}^{n_r \times \hat{n}}$. The realization $(\hat{\mathbf{E}}, \hat{\mathbf{A}}, \hat{\mathbf{B}}, \hat{\mathbf{C}})$ of reduced order $\hat{n}$, follows from Eq. 7 where $\mathbf{Y} = \hat{\mathbf{Y}}$, $\mathbf{X} = \hat{\mathbf{X}}$. Associated rational matrix approximates the sampled data along the tangential directions with some approximation error. To avoid high approximation errors, $\hat{n}$ is chosen such that the $\hat{n}$th singular value $\sigma_{\hat{n}}$ of $(\mathbb{L}_\sigma, \mathbb{L})$ is sufficiently small.

3.3 Parametric Loewner Framework

The non-parametric Loewner framework presented in Subsection 3.2 is not suitable for modeling parameter-dependent systems, such as aerodynamic systems, since it requires a new calculation of input data with each change in parameter value. This implies high computational costs and time inefficiency. Therefore, simulation, optimization, and control design require a parametric framework which generates the state-space realization for an arbitrary value of parameter p, from a single sampled set. In this work, a single parameter is considered.

Parametric generalized realization refers to the modeling of transfer function/matrix data sampled at N complex variable values and P parameter variable values,

$$\{s_i, p_l, \boldsymbol{\Phi}_{il} \mid s_i \in \mathbb{C}, p_l \in \mathbb{R}, \boldsymbol{\Phi}_{il} \in \mathbb{C}^{n_y \times n_u}\}_{i=1,l=1}^{N,P}, \tag{9}$$

with a parametric descriptor system,

$$\Sigma(p): \begin{aligned} \mathbf{E}(p)\dot{\mathbf{x}}(t) &= \mathbf{A}(p)\mathbf{x}(t) + \mathbf{B}(p)\mathbf{u}(t) \\ \mathbf{y}(t) &= \mathbf{C}(p)\mathbf{x}(t) + \mathbf{D}(p)\mathbf{u}(t), \end{aligned}$$

where the state-space matrices are functions of p, such that $\tilde{\mathbf{H}}(\Sigma)(s_i, p_l) = \boldsymbol{\Phi}_{il}$.

Transfer matrix interpolation The first approach based on transfer matrix interpolation does not fit the above definition since the state-space matrices are not given with an explicit dependence on p. However, this approach allows the generation of a descriptor system for an arbitrary parameter value $p = const.$, using a single sampled set (Eq. 9). This is done in two steps. First, the values of transfer matrix for a chosen $p = const.$ are calculated by interpolating the samples given with Eq. 9 in p for each value of the complex variable s_i,

$$\boldsymbol{\Phi}_{int_i}(p) = \sum\nolimits_{l=1}^{P} \boldsymbol{\Phi}_{il}\varphi_l(p),$$

where φ_l depends on the interpolation technique. The interpolated transfer matrix forms a new, interpolated set, $\{s_i, \ \boldsymbol{\Phi}_{int_i}(p) \mid s_i \in \mathbb{C}, \ \boldsymbol{\Phi}_{int_i}(p) \in \mathbb{C}^{n_y \times n_u}\}, \ i = 1 : N$. Reduced-order realization $(\hat{\mathbf{E}}, \hat{\mathbf{A}}, \hat{\mathbf{B}}, \hat{\mathbf{C}})(p = const.)$ for the chosen value of p, which closely approximates the interpolated data $\boldsymbol{\Phi}_{int}(p = const.)$, is then built with the non-parametric Loewner framework from Subsection 3.2. The resulting state-space matrices are constant matrices and thus a new realization needs to be built for each fixed parameter value of interest. This limitation can be overcome with the global basis approach.

Global basis approach The global basis approach, introduced in Yue et al. (2019), allows the generation of a parametric descriptor system with state-space matrices given as functions of a parameter. First, the sampled set (Eq. 9) is augmented with the set of left and right tangential directions, $\mathbf{r}_j$ and $\boldsymbol{\ell}_i$, constant for all parameter values. The data is then partitioned into two disjoint sets for each parameter value from the sampled set, $p_l, l = 1 : P$,

$$\{\lambda_j, \mathbf{r}_j, \mathbf{w}_j(p_l), j = 1 : n_r\} \cup \{\mu_i, \boldsymbol{\ell}_i, \mathbf{v}_i(p_l), i = 1 : n_l\}.$$

The non-parametric realization $(\mathbf{E}, \ \mathbf{A}, \ \mathbf{B}, \ \mathbf{C})(p_l)$ is built for each parameter value, $p_l, l = 1 : P$, using the non-parametric Loewner realization based on the tangential interpolation (Subsection 3.2). Finally, the realization for an arbitrary value of p is found by interpolating the non-parametric state-space matrices,

$$\mathbf{\Psi}(p) = \sum_{l=1}^{P} \mathbf{\Psi}(p_l)\varphi_l(p), \quad \mathbf{\Psi} \in \{\mathbf{E},\ \mathbf{A},\ \mathbf{B},\ \mathbf{C}\}. \quad (10)$$

The interpolation of state-space matrices is only possible if the matrices are of the same size. This always holds for the realizations given in the full form (Eq. 8). However, the full-form realizations are usually of high order. Therefore, to make sure that all local matrices are of low order and compatible for interpolation, order reduction is done by projecting the systems onto the same basis. It is proven in Yue et al. (2019) that the left singular vectors $\mathbf{Y}_g$ of the horizontal global Loewner pencil $[s_i\mathbb{L}(p_1) - \mathbb{L}_\sigma(p_1)\ \dots\ s_i\mathbb{L}(p_P) - \mathbb{L}_\sigma(p_P)]$ and the right singular vectors $\mathbf{X}_g$ of the vertical global Loewner pencil $[(s_i\mathbb{L}(p_1) - \mathbb{L}_\sigma(p_1))^*\ \dots\ (s_i\mathbb{L}(p_P) - \mathbb{L}_\sigma(p_P))^*]^*$ span the whole vector subspace which contains all local singular vectors. Therefore, the basis for reduction of all local systems are chosen as the $\hat{n}$ most dominant left and right global singular vectors, $\hat{\mathbf{Y}}_g$ and $\hat{\mathbf{X}}_g$. Local realizations $(\hat{\mathbf{E}},\ \hat{\mathbf{A}},\ \hat{\mathbf{B}},\ \hat{\mathbf{C}})(p_l)$, $l = 1 : P$, of reduced order $\hat{n}$ follow from Eq. 7 with $\mathbf{Y} = \hat{\mathbf{Y}}_g$, $\mathbf{X} = \hat{\mathbf{X}}_g$. Finally, realization of the same reduced order $\hat{n}$ for any parameter value p can be obtained by interpolation (Eq. 10). Unlike the transfer matrix interpolation, this method does not require a new realization for each new parameter value, but only interpolation of already built state-space matrices. However, common tangential directions and order $\hat{n}$ are required for all local realizations. The latter can result in non-minimal realizations when the samples originate from a rational matrix, while for non-rational samples, the recovered realizations are usually minimal. Furthermore, unique settings can be unsuitable for the data which is drastically changing within the parameter range of interest, in which case the transfer matrix interpolation is preferred.

4. AERODYNAMIC MODELING

Now, let us discuss the approach used to model unsteady aerodynamic loads. First, the descriptor system of reduced order,

$$\hat{\Sigma}_a(M): \begin{aligned} \hat{\mathbf{E}}(M)\dot{\mathbf{x}}(t) &= (U/b)\hat{\mathbf{A}}(M)\mathbf{x}(t) + \hat{\mathbf{B}}(M)\boldsymbol{\xi}(t) \\ \mathbf{Q}_a(t, M) &= (U/b)\hat{\mathbf{C}}(M)\mathbf{x}(t), \end{aligned} \quad (11)$$

is built from a set of scaled aerodynamic transfer matrix data, $\{\imath k_i, M_j, \bar{\mathbf{H}}_{a_{ij}}\}_{i=1,j=1}^{N,P}$, by applying the parametric Loewner frameworks presented in Subsection 3.3. The associated transfer matrix, $\tilde{\mathbf{H}}(\hat{\Sigma}_a)(\bar{s}, M) = \hat{\mathbf{C}}(M)(\bar{s}\hat{\mathbf{E}}(M) - \hat{\mathbf{A}}(M))^{-1}\hat{\mathbf{B}}(M)$, is allowed to be improper for some M (when $\hat{\mathbf{E}}(M)$ is singular). This is suitable for interpolating the sampled data since the unbounded behavior of the aerodynamic loads, captured with the used aerodynamic solver, can be modeled. Furthermore, the framework is based on interpolation and allows for reduction of order without introducing large approximation errors. Finally, using the parametric formulation of the framework, dynamic behavior of the aerodynamic system can be evaluated for any Mach number value without recalculating the airloads. However, since the matrix $\hat{\mathbf{E}}$ is singular, or often close to singular due to the nature of the Loewner matrix, the state-space equations are given in differential algebraic equation (DAE) form. DAEs are computationally inefficient and expensive to solve, thus not suitable for control design. Furthermore, the Loewner framework does not guarantee preservation of asymptotic stability which is inherent to the observed aerodynamic system. Therefore, post-processing techniques for reduction of the system to stable ODE form, described with Eq. 3, are applied.

4.1 Reduction to Stable ODE Form

Here, a modified version of the approach used in Quero et al. (2019) for the reduction of $\hat{\Sigma}_a(M)$ (Eq. 11) to stable ODE form (Eq. 3) is implemented. First, the transfer matrix of the descriptor system $\hat{\Sigma}_a(M)$ is evaluated for some value $M = const.$ (in the case of global basis approach) and split into a strictly-proper and a polynomial part by vector fitting. The latter is done by approximating each entry of the transfer matrix with a rational function which has a polynomial part of second degree,

$$[\tilde{\mathbf{H}}]_{ij}(\hat{\Sigma}_a)(\bar{s}) \approx [\mathbf{D}_{a0}]_{ij} + [\mathbf{D}_{a1}]_{ij}\bar{s} + [\mathbf{D}_{a2}]_{ij}\bar{s}^2 + \sum_{l=1}^{n_f} \frac{[\mathbf{R}_l]_{ij}}{\bar{s} - \bar{\rho}_l}$$

where residues $[\mathbf{R}_l]_{ij}$ and polynomial coefficients $[\mathbf{D}_a]_{ij}$ are calculated with the least-squares technique. Unlike in the original vector fitting method (Gustavsen and Semlyen (1999)), poles $\bar{\rho}_l$ are known from the generalized realization with the Loewner framework, $\bar{\rho}_l \in \Lambda(\hat{\mathbf{A}}, \hat{\mathbf{E}})$, $\bar{\rho}_l < |\bar{\rho}_\infty|$. Note that only finite poles need to be chosen. Furthermore, the unstable poles are replaced with their counterparts mirrored through the imaginary axis. Given the set of poles $\bar{\rho}_l$ and the residues $\mathbf{R}_l$, minimal realization $(\mathbf{A}_a, \mathbf{B}_{a0}, \mathbf{C}_a)$ of the strictly-proper transfer matrix part is found by means of Gilbert realization (see Gilbert (1963)). Finally, given the polynomial matrices $(\mathbf{D}_{a0}, \mathbf{D}_{a1}, \mathbf{D}_{a2})$ and the realization of the strictly-proper part, a stable state-space system S_a in ODE form (Eq. 3) can be formulated. This approach yields models less sensitive to the tolerance $|\bar{\rho}_\infty|$ (more robust) than the approaches used in Quero et al. (2019) and Vojković (2021). Additionally, no post-processing stabilization technique is needed.

4.2 Numerical settings

All settings for the application of the parametric Loewner frameworks to unsteady aerodynamic modeling are chosen based on the analysis of the approximation error and the order of system. This analysis is not shown here due to space limitations. The aerodynamic transfer matrix is sampled for $N = 31$ logarithmically spaced points on the range $k \in \left[10^{-6}, 2.2\right]$. For both methods, Lagrange polynomial interpolation is chosen as the interpolation technique. To avoid Runge effect, sampling of the transfer matrix in Mach number is logarithmic with higher density of sampling points at the edges of the observed interval. The total number of Mach number sample points is $P = 19$. Tangential directions are constructed from singular vectors of sampled, in the case of global basis approach, or interpolated transfer matrices, in the case of transfer matrix interpolation, as explained in Vojković (2021). Tolerance for the smallest normalized singular value of the Loewner pencil which is not truncated is chosen to be $\sigma_{\hat{n}}/\sigma_1 = 10^{-5}$ for the global basis approach and $\sigma_{\hat{n}}/\sigma_1 = 10^{-6}$ for the transfer matrix interpolation approach (for all Mach numbers). These values give a good ratio of order and accuracy of the system. Due to the robustness of the approaches, a common tolerance of $|\bar{\rho}_\infty| = 2$ for infinite poles is used for all models in both approaches.

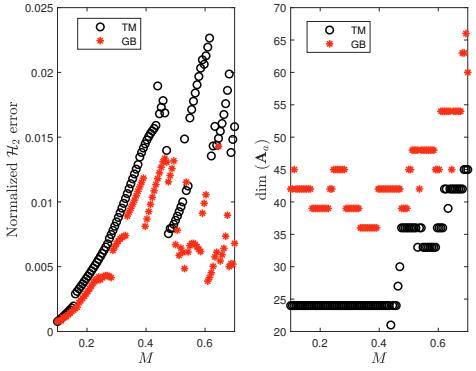

Fig. 2: Normalized $\mathcal{H}_2$ norms of pointwise system errors and orders of systems obtained with transfer matrix interpolation (TM) and the global basis (GB) approach.

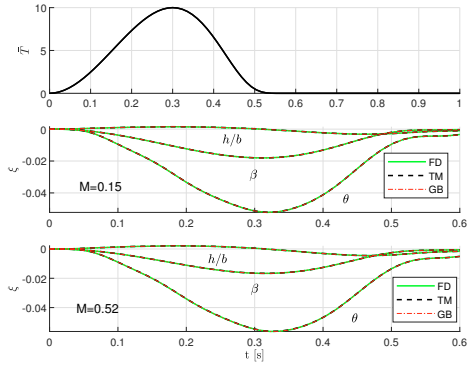

Fig. 3: Structural and control surface displacements due to the pulse excitation in $\bar{T}$ predicted with state-space models, obtained with transfer matrix interpolation (TM) and global basis (GB) approach. Frequency domain (FD) responses are shown as a reference.

5. EVALUATION OF AEROELASTIC MODELS

Finally, analysis of the constructed aerodynamic and aeroelastic state-space systems is given. First, the accuracy and order of the aerodynamic models is analyzed. Fig. 2 shows the normalized $\mathcal{H}_2$ norm of the pointwise system error (see Lefteriu and Antoulas (2009)) which is evaluated for 100 linearly spaced Mach numbers on the observed range. Reference values are obtained with the potential aerodynamic solver as explained in Section 2. The orders of the constructed systems are shown as well. It can be seen that, for the given settings, the global basis approach gives slightly more accurate models than the transfer matrix interpolation approach. However, the overall accuracy of both methods is high. The orders of the systems are however significantly higher for the global basis approach.

Next, the dynamic behavior of the aeroelastic state-space systems is evaluated for the input $\bar{T}(t)$ given as:

$$\bar{T}(t) = 4(t/t_0)^2 e^{(2-1/(1-t/t_0))}, \ 0 \leq t \leq t_0,$$
$$\bar{T}(t) = 0, \ t > t_0,$$

where $t_0 = 0.6$ $[s]$. Structural displacements are obtained by solving the set of ODEs (Eq. 2) with an ODE solver of fifth order, using the fixed time step $\Delta t = 0.012$ $[s]$ and setting the initial conditions to zero. The results are validated with the frequency domain solutions, which are obtained by solving the EOM (Eq. 1) in the frequency domain and applying the inverse fast Fourier transform. This allows calculation of the structural displacements with the reference values of aerodynamic loads. The results are shown for Mach numbers $M = 0.15$ and $M = 0.52$, not included in the sampled set, in Fig. 3. It can be concluded that the state-space models obtained with both approaches accurately capture the reference dynamic behavior.

REFERENCES

EASA (2015). Ceritification Specifications and Acceptable Means of Compliance for Large Aeroplanes. Technical Report CS-25, European Aviation Safety Agency.

Gilbert, E.G. (1963). Controllability and observability in multivariable control systems. *Journal of the Society for Industrial and Applied Mathematics, Series A: Control*, 1(2), 128–151.

Gustavsen, B. and Semlyen, A. (1999). Rational Approximation of Frequency Domain Responses by Vector Fitting. *IEEE Transactions on power delivery*, 14(3), 1052–1061.

Ionita, A.C. (2013). *Lagrange Rational Interpolation and its Applications to Model Reduction and System Identification*. Ph.D. thesis, Rice University.

Ionita, A.C. and Antoulas, A.C. (2014). Data-Driven Parametrized Model Reduction in the Loewner Framework. *SIAM Journal on Scientific Computing*, 36(3), A984–A1007.

Irving, A. (1979). An Analytical Technique for Predicting the Characteristics of a Flexible Wing Equipped with an Active Flutter-Suppression System and Comparison with Wind-Tunnel Data. Technical Report 1367, National Aeronautics and Space Administration.

Lefteriu, S. and Antoulas, A. (2009). A New Approach to Modeling Multiport Systems From Frequency-Domain Data. *IEEE Transactions on Computer-Aided Design of Integrated Circuits and Systems*, 29(1), 14–27.

Marques, A. (2019). Python Code for Solving Possio Integral Equation. URL `https://github.com/anmarques/DLM2D`.

Mayo, A.J. and Antoulas, A.C. (2007). A Framework for the Solution of the Generalized Realization Problem. *Linear Algebra and its Applications*, 425(2-3), 634–662.

Quero, D., Vuillemin, P., and Poussot-Vassal, C. (2019). A Generalized State-Space Aeroservoelastic Model Based on Tangential Interpolation. *Aerospace*, 6(1), 9.

Quero, D., Vuillemin, P., and Poussot-Vassal, C. (2021). A generalized eigenvalue solution to the flutter stability problem with true damping: The p-L method. *Journal of Fluids and Structures*, 103.

Roger, K.L. (1977). Airplane Math Modeling Methods for Active Control Design. In *Proceedings of the 44th AGARD Structures and Material Panel Conference*.

Theodorsen, T. (1935). General Theory of Aerodynamic Instability and the Mechanism of Flutter. Technical Report 496, NASA.

Vojković, T. (2021). *Generalized State-Space Realization of Parameter-Dependent Unsteady Aerodynamic Models*. Master's thesis, Delft University of Technology.

Yue, Y., Feng, L., and Benner, P. (2019). Reduced-Order Modelling of Parametric Systems via Interpolation of Heterogeneous Surrogates. *Advanced Modeling and Simulation in Engineering Sciences*, 6(1), 1–33.